Journal of Bio- and Tribo-Corrosion (2019) 5:8
https://doi.org/10.1007/s40735-018-0202-8

Corrosion Inhibition of Mild Steel in 0.5 M H_2SO_4 Solution by *Artemisia herba-alba* Oil

K. Boumhara[1] · H. Harhar[1] · M. Tabyaoui[1] · A. Bellaouchou[1] · A. Guenbour[1] · A. Zarrouk[1]

Received: 25 April 2018 / Revised: 24 October 2018 / Accepted: 13 November 2018 / Published online: 19 November 2018

Abstract
Artemisia herba-alba oil (AHAO) was obtained by hydrodistillation of the aerial parts of the plant and analyzed by GC and GC–MS. AHAO was tested as corrosion inhibitor of mild steel in 0.5 M H_2SO_4 solution using weight loss measurement and the stationary polarization curves. Results obtained indicate that the corrosion rate is reduced and AHAO adsorbs on the metal surface and then inhibits corrosion process. The highest inhibiting efficacy reached 88% at 298 K at 2.76 g L^{-1}. The influence of the temperature (303–343 K) on the inhibition efficacy at different concentrations of AHAO was investigated. Thermodynamic data for AHAO inhibitor adsorption and mild steel corrosion led to suggest the occurrence of comprehensive adsorption physical adsorption for the inhibitor species on mild steel.

Keywords *Artemisia herba-alba* · Mild steel · Corrosion inhibition · H_2SO_4 · Adsorption

1 Introduction

Artemisia herba-alba (AHA) greenish-silver perennial herb grows 20–40 cm in height and belongs to the daisy family Asteraceae [1]. This plant usually renowned in Morocco as "Chih" and in France as "Armoise balnche" [2]. It has been utilized in popular medicine by many cultures since antique times, to treat colds, coughing, bronchitis, intestinal disturbances, diarrhea, neuralgias arterial hypertension, and/or diabetes [3–5]. Over the last decades, studies on AHA were focused on its essential oils. Their content through the world indicated a high level of polymorphism and guided to the definition of various chemotypes [6]. Many investigators have reported miscellaneous biological and/or pharmacological activities of AHA essential oil as an antimicrobial, antidiabetic, antioxidant, anthelmintic, Antileishmanial, and antispasmodic agent [1, 7–10].

Mild steel has widespread industrial applications due to their availability and low cost. In processes such as acid cleaning, pickling, and descaling operations in oil and gas exploration, acidic solutions are widely used. Mild steel surfaces exert in service in these environments which undergo considerable corrosion. Significant reduction in corrosion rates has been attained by various means inclosed reduction of the mild steel impurity content, application of several surface modification techniques as well as insertion of desirable alloying elements [11]. However, the preventions used to reduce the corrosion of materials include those related to the use of corrosion inhibitors, and the choice of appropriate inhibitors is dependent primarily on the structure. Most of these inhibitors are organic molecules which generally include heteroatoms, π-electron, and aromatic rings, which allow an adsorption on the metal surface [12–17]. These inhibitors are adsorbed on the metal surface and block active corrosion sites, and the majority of them are toxic to humans and their environment. Hence, the use of natural products as eco-friendly and harmless corrosion inhibitors has become popular [18–23]. These inhibitory substances can beget temporary or permanent damage to organs such as the kidneys or liver, or disrupt the enzymatic system in the body. The toxicity can occur either during the synthesis of these compounds or during their applications. As a result, natural substances are increasingly seen as an alternative to these synthetic inhibitors, which are environmentally friendly and safe. Inhibitors of natural origin are utilized for the protection of metals in the acid environment, in order to replace the toxic chemicals currently utilized [24, 25].

In the present work, the chemical composition of *Artemisia herba-alba* essential oil (AHAO) is established using

✉ A. Zarrouk
azarrouk@gmail.com

[1] Laboratory of Materials, Nanotechnology and Environment, Faculty of Sciences, Mohammed V University, Av. Ibn Battuta, B.P 1014 Rabat, Morocco

GC and GC–MS. Corrosion inhibition efficiency has been experimentally evaluated using gravimetric and polarization methods. The effect of temperature on the corrosion behavior of mild steel in 0.5 M H_2SO_4 with the addition of AHAO was studied in the temperature range of 298–343 K. The adsorption and kinetic parameters for mild steel/AHAO/0.5 M H_2SO_4 system were calculated from experimental gravimetric data and the interpretation of the results is given. Scanning electron microscopy (SEM) has been applied to study the mechanism of mild steel corrosion inhibition of this essential oil in acidic medium.

2 Experimental Procedures

2.1 Plant Collection and Essential Oil Extraction

Artemisia herba-alba was harvested in Mars 2008 from the garden of the reserve area of Boulemane locality in Morocco. The collection of the plant and the extraction of the essential oil was made according to the same protocol described in a previously published work [26].

2.2 Gas Chromatography Analysis (GC–FID) and Gas Chromatography Mass Spectrometry (GC–MS)

GC–FID, GC–MS, and the identification of the essential oil constituents were made according to previously published works [26].

2.3 Components Identification

The identification of the essential oil constituents was based on (i) comparison with the mass spectra of authentic reference compounds where possible and by reference to WILEY275, NIST 02, and Adams mass spectral libraries [27], (ii) comparison of their retention index (RI), calculated relative to the retention times of a series of C-5 to C-30 n-alkanes, with linear interpolation, with those of our own library of authentic compounds or literature data [27, 28].

2.4 Corrosion Tests

Mild steel (C: 0.21, Mn: 0.05, Si: 0.38, S: 0.05, P: 0.09, Al: 0.01, and the remainder iron) was utilized. Prior to each experiment, the mild steel specimen was abraded with a series of emery paper from 400 to 1200 grades. The specimen was washed several times with distilled water, then with ethanol, and finally dried using a stream of air.

The acidic solution 0.5 M H_2SO_4 was prepared by dilution of Analytical Grade H_2SO_4 with distilled water. The concentration range of AHAO in these dilute solutions was from 0.65 to 2.76 g L^{-1}.

Gravimetric methods are carried out in a double-walled glass cell equipped with a thermostated cooling condenser. The solution volume is 50 mL. The steel specimens utilized have rectangular shapes 3 cm × 1 cm × 0.1 cm. For each sample, three tests are realized and the corresponding average value is calculated. The samples were weighted with an uncertainty of 10^{-4} g. The immersion time for weight loss amounts is 6 h for all the temperatures.

2.5 Polarization Measurements

Polarization curves were conducted using an electrochemical measurement system Voltalab 40 potentiostat–galvanostat (Radiometer Analytical PGZ 301) and controlled with corrosion analysis software VoltMaster 4.0. The working electrode (WE) in the form of disc cut from steel has a geometric area of 1 cm^2 and is embedded in polytetrafluoroethylene (PTFE). A saturated calomel electrode (SCE) and a platinum electrode were utilized, as reference and auxiliary electrodes, respectively. The WE was immersed in test solutions for 30 min to establish steady-state open circuit potential (E_{ocp}) by applying 10 mV ac voltage peak-to-peak. After measuring the E_{ocp}, the electrochemical measurements were performed. All electrochemical tests have been performed in aerated solutions at 298 K. The potential was swept to anodic potentials by a constant sweep rate of 0.5 mV s^{-1} and potential was scanned in the range of − 800 to 0 mV/SCE relative to the corrosion potential.

3 Results and Discussion

3.1 Analysis of *Artemisia herba-alba* Essential Oil

The analysis of essential oil from AHA was carried out by CG/FID and CG/MS. The chemical composition of essential oil was characterized by 24 compounds, which accounted for 98.4% of the total oil. The retention time of volatile compounds (RIa and RIp) and their percentage are summarized in Table 1. The oil was dominated by oxygenated monoterpenes (70.2%) followed by monoterpenic hydrocarbons (26.6%). The sesquiterpene hydrocarbons and oxygenated sesquiterpenes accounted only for 1.6%. The essential oil was characterized by high amounts of 1,8-Cineole (35.6%). The other major components were camphor (24.1%), α-Pinene (11.6%), and Camphene (4.9%). The 24 other compounds are reported in low amounts in AHA essential oil from Morocco. It should be noted that several studies have been published on chemical composition of AHA in Mediterranean basin. The study made by Boutkhil et al. [29] on the regions of Oujda and Errachidia showed that the composition of the AHAO from Oujda was rich in α-thujone (46.75%), β-thujone (21.17%), and camphor

Table 1 Chemical composition (%) of the Essential oils from *Artemisia herba-alba*

N°	Compounds	Ir (apol)	Ir (pol)	*Artemisia herba-alba*
1	Tricyclene	921	1011	0.2
2	α-Thujene	923	1024	0.1
3	α-Pinene	933	1024	11.6
4	Camphene	945	1069	4.9
5	1-Octen-3-ol	962	1441	0.2
6	β-Pinene	972	1112	4.1
7	Myrcene	982	1132	0.8
8	Yomogi alcohol	985	1391	0.1
9	p-Cymene	1013	1268	1.8
10	1,8-Cineole	1023	1212	35.6
11	Limonene	–	1202	1.8
12	γ-Terpinene	1049	1243	0.2
13	Terpinolene	1080	1281	0.1
14	α-Thujone	1085	1394	1.1
15	Linalool	1088	1538	1.4
16	β-Thujone	1099	1434	0.4
17	Camphor	1126	1510	24.1
18	δ-Terpineol	1149	1659	0.5
19	Borneol	1152	1689	3.6
20	Terpinen-4-ol	1163	1591	0.8
21	α-Terpineol	1174	1685	2.9
22	Bornyl acetate	1270	1573	0.5
23	E-caryophyllene	1417	1591	1.2
24	α-Humulene	1450	1661	0.4
Total				98.4

All the values are mean ± SD

SD standard deviation, *RI a* retention indices on the apolar column (Rtx-1), *RI p* retention indices on the polar column (Rtx-Wax)

(8.41%), the essential oil from Errachidia was rich in camphor (17.79%), α-thujone (17.27%), the cis-chrysanthenyl acetate (10.9%), β-thujone (9.91%), davanone (6.65%), the chrysanthenone (6.37%), and the eucalyptol (4.98%), and the difference observed in the chemical composition of AHA for the same country can be explained by the techniques utilized for the extraction.

3.2 Gravimetric Measurements

3.2.1 Effect of AHAO Concentration

The effect of addition of AHAO tested at different concentrations on the corrosion of mild steel in 0.5 M H_2SO_4 solution was studied by weight loss measurements at 298 K after 6 h of immersion period. The corrosion rate (C_R) and inhibition efficacy η(%) were calculated according to the Eqs. 1 and 2 [30], respectively:

Table 2 Gravimetric results of mild steel in 0.5 M H_2SO_4 at different concentrations of AHAO during 6 h at 298 K

Medium	C (g L^{-1})	C_R (mg cm^{-2} h^{-1})	η_{WL} (%)
Blank	0	3.133	–
AHAO	0.65	0.722	77
	1.20	0.672	79
	1.57	0.619	80
	1.84	0.531	83
	2.76	0.467	85

$$C_R = \frac{W_b - W_a}{At} \quad (1)$$

$$\eta_{WL}(\%) = \left(1 - \frac{w_i}{w_0}\right) \times 100, \quad (2)$$

where W_b and W_a are the specimen weight before and after immersion in the tested solution, w_0 and w_i are the values of corrosion weight losses of mild steel in uninhibited and inhibited solutions, respectively, A the area of the mild steel specimen and t is the exposure time (h).

The weight loss data are given in Table 2.

It is very clear from this table that the corrosion rate increased with the decreased with inhibitor concentration. This phenomenon is caused by the adsorption of active molecules of *Artemisia herba-alba oil* (AHAO) on the mild steel surface. The highest value of inhibition efficacy is obtained at 2.76 g L^{-1} (by weight) inhibitor concentration.

3.2.2 Effect of the Temperature

The effect of temperature on the inhibited acid–metal reaction is very complex, because many changes occur on the metal surface such as rapid etching, desorption of inhibitor, and the inhibitor itself may undergo decomposition. The change of the corrosion rate at selected concentrations of the AHAO during 6 h of immersion with the temperature was studied in 0.5 M H_2SO_4, both in the absence and presence of AHAO. For this purpose, gravimetric experiments were performed at different temperatures (303–343 K) and the results are given in Table 3.

The obtained data in Table 3 reveal that the inhibition efficacy increased with an increase in the AHAO concentration. This suggests that the AHAO species are adsorbed on the mild steel/solution interface where the adsorbed species mechanically screen the coated part of the metal surface from the action of the corrosive medium.

As observed from Table 3, the effect of temperature on the inhibition efficacy of the studied AHAO at all concentrations and temperatures shows that a remarkable decrease in the AHAO efficacy was observed with increasing temperature

Table 3 The effect of AHAO concentration on the weight loss of mild steel in 0.5 M H_2SO_4 solution

T (K)	C (g L^{-1})	C_R (mg cm^{-2} h^{-1})	η_{WL} (%)
303	Blank	4.247	–
	0.65	0.942	78
	1.20	0.804	81
	1.57	0.714	83
	1.84	0.610	85
	2.76	0.530	87
313	Blank	6.167	–
	0.65	1.583	74
	1.20	1.078	82
	1.57	0.967	84
	1.84	0.856	86
	2.76	0.739	88
323	Blank	10.925	–
	0.65	4.769	56
	1.20	3.425	69
	1.57	3.022	72
	1.84	2.717	75
	2.76	2.317	79
333	Blank	16.456	–
	0.65	10.3	37
	1.20	8.336	49
	1.57	7.227	56
	1.84	6.844	58
	2.76	6.301	62
343	Blank	21.372	–
	0.65	16.183	24
	1.20	13.630	36
	1.57	12.489	42
	1.84	11.967	44
	2.76	10.953	49

up to 343 K. This variation of the efficacy versus temperature shows that physisorption mechanism is effectively enhanced with rising temperature.

The effect of temperature on the inhibited acid-metal reaction is highly complex, this is due to the change that occurs on the metal surface such as rapid etching and desorption of AHAO. Also the inhibitor itself may undergo decomposition and/or rearrangement [31]. However, it was found that few inhibitors with acid-metal systems have specific reactions which are effective at high temperature as (or more) they are at low temperature [32, 33].

To calculate activation thermodynamic parameters of the corrosion process, Arrhenius Eq. (3) and transition state Eq. (4) were utilized [34]:

$$C_R = A \exp\left(-\frac{E_a}{RT}\right) \tag{3}$$

$$C_R = \frac{RT}{Nh} \exp\left(\frac{\Delta S_a}{R}\right) \exp\left(-\frac{\Delta H_a}{RT}\right), \tag{4}$$

where E_a is the apparent activation corrosion energy, R is the universal gas constant, A is the Arrhenius pre-exponential factor, h is Plank's constant, N is Avogadro's number, ΔS_a is the entropy of activation, and ΔH_a is the enthalpy of activation.

Arrhenius plots for the corrosion rate of mild steel [Ln(C_R) vs. 1/T] are given in Fig. 1. Values of apparent activation energy of corrosion (E_a) for mild steel in 0.5 M H_2SO_4 with the absence and presence of various concentrations of AHAO are calculated by linear regression between Ln(C_R) and 1/T and the results are given in Table 4.

All the linear regression coefficients are close to 1, indicating that the mild steel corrosion in 0.5 M H_2SO_4 can be elucidated using the kinetic model. As observed from the Table 4, the E_a increased with increasing concentration of

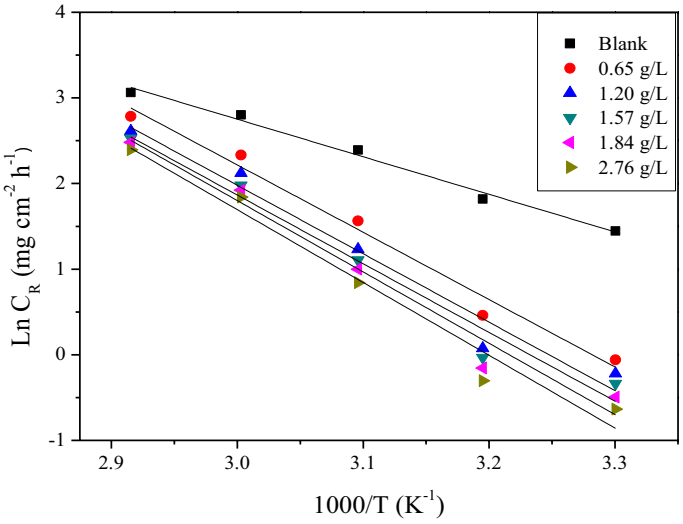

Fig. 1 Arrhenius plots for mild steel corrosion rates (C_R) in 0.5 M H_2SO_4 in the absence and in presence of different concentrations of AHAO

Table 4 Kinetic-thermodynamic corrosion parameters for mild steel corrosion in the absence and presence of various concentrations of AHAO

C (g L^{-1})	E_a (KJ mol^{-1})	ΔH_a (KJ mol^{-1})	$-\Delta S_a$ (KJ $mol^{-1}K^{-1}$)
Blank	36.5	33.9	0.209
0.65	65.4	62.7	0.126
1.20	67.9	65.9	0.121
1.57	69.9	67.2	0.116
1.84	74.1	71.4	0.104
2.76	77.2	74.5	0.095

AHAO, but all values of E_a in the range of the studied concentration were higher than that of the uninhibited solution (blank). The increase in E_a in the presence of AHAO may be interpreted as physical adsorption. Indeed, a higher energy barrier for the corrosion process in the inhibited solution is associated with physical adsorption or weak chemical bonding between the inhibitor species and the steel surface [13, 35]. Szauer et al. explained that the increase in activation energy can be attributed to an appreciable decrease in the adsorption of the inhibitor on the mild steel surface with the increase in temperature. A corresponding increase in the corrosion rate occurs because of the greater area of metal that is consequently exposed to the acid environment [36].

Figure 2 shows a plot of Ln (C_R/T) against 1/T. Straight lines are obtained with a slope of ($-\Delta H_a/R$) and an intercept of (Ln $R/Nh + \Delta S_a/R$) from which the values of ΔH_a and ΔS_a are calculated, and are listed in Table 4.

Inspection of these data reveals that the ΔH_a values for dissolution reaction of mild steel in 0.5 M H_2SO_4 in the presence of AHAO are higher (62.7–74.5 kJ mol^{-1}) than that of in the absence of AHAO (36.5 kJ mol^{-1}). The positive signs of ΔH_a values reflect the endothermic nature of the mild steel dissolution process suggesting that the dissolution of mild steel is slow [37] in the presence of inhibitor. All values of E_a are larger than the analogous values of ΔH_a indicating that the corrosion process must involve a gaseous reaction, simply the hydrogen evolution reaction, associated with a decrease in the total reaction volume [24].

From Table 4, it is clear that the increase in AHAO concentration leads to an increase in entropy. The increase of ΔS_a is generally interpreted as an increase in disorder as the reactants are converted to the activated complexes [30]. This observation is in agreement with the findings of other workers [38–41]. This behavior can also be explained as a result of the replacement process of water molecules during adsorption of AHAO molecules on the steel surface and therefore the increase in entropy of activation was attributed to the increasing in solvent entropy [42].

3.3 Adsorption Isotherms

The extent of inhibitive actions of the studied compounds has been expanded in terms of the adsorption mode of the inhibitor. An efficient organic corrosion inhibitor is expected to adhere onto the metal surface immersed in aqueous solution via a quasi-substitution mode [43, 44]. A correlation between surface coverage (θ) defined by η%/100 obtained from weight loss and the concentrations of AHAO (C_{inh}) was fitted to Langmuir and Temkin adsorption isotherms. Both isotherms are presented in Figs. 3 and 4, and the mathematical forms of the isotherms employed are

$$\text{Langmuir}: \frac{C}{\theta} = \frac{1}{K} + C \tag{5}$$

$$\text{Temkin}: Ln\left(\frac{\theta}{C}\right) = LnK - g\theta, \tag{6}$$

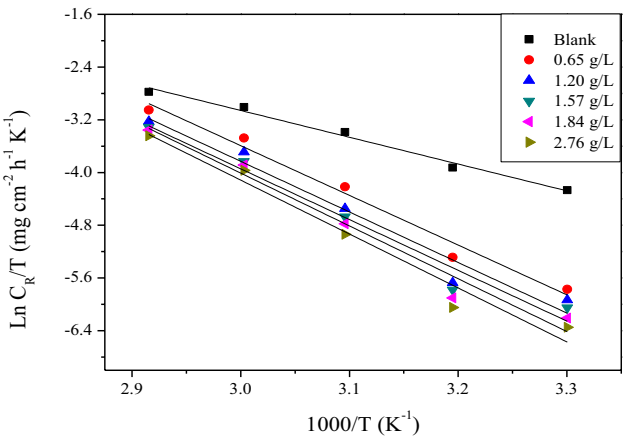

Fig. 2 Transition state plots for mild steel corrosion rates (C_R) in 0.5 M H_2SO_4 in the absence and presence of different concentrations of AHAO

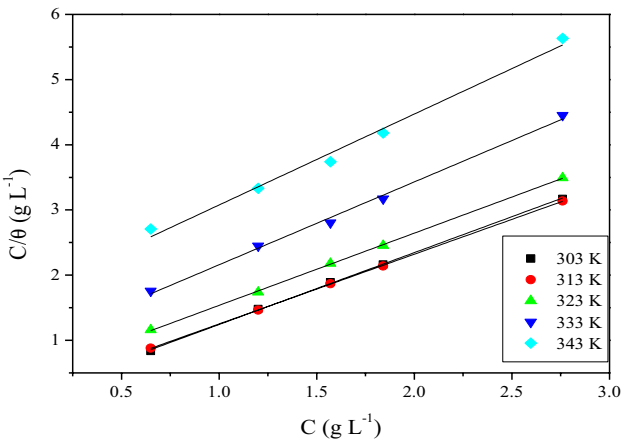

Fig. 3 Langmuir's isotherm adsorption model of AHAO on the mild steel surface in 0.5 M H_2SO_4 at different temperatures

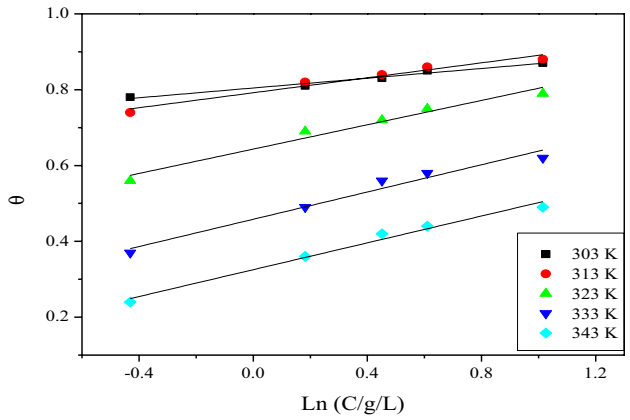

Fig. 4 Temkin isotherm adsorption model of AHAO on the mild steel surface in 0.5 M H_2SO_4 at different temperatures

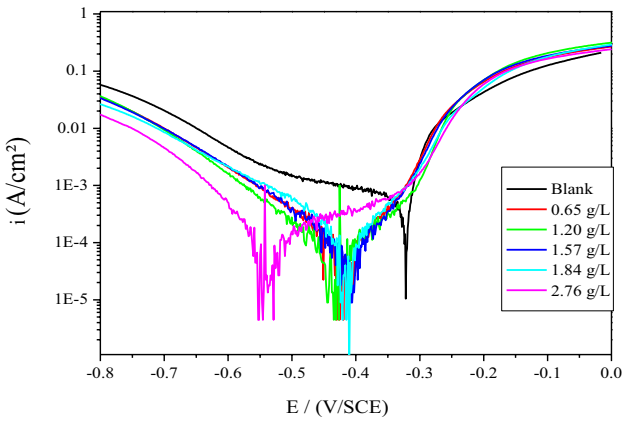

Fig. 5 Polarization curves of steel in 0.5 M H_2SO_4 in the presence of different concentrations of AHAO at 298 K of the corrosive medium

Table 5 Adsorption parameters for AHAO in 0.5M H_2SO_4 obtained from Langmuir and Temkin adsorption isotherms at different temperatures

T (K)	Slope	Intercept	R^2
Langmuir			
303	1.1029	0.1396	0.9994
313	1.0694	0.1819	0.9999
323	1.1083	0.4278	0.9996
333	1.2707	0.8885	0.9948
343	1.3950	1.6813	0.9870
Temkin			
303	0.0642	0.8045	0.9724
313	0.0987	0.7919	0.9530
323	0.1605	0.6433	0.9624
333	0.1798	0.4583	0.9611
343	0.1769	0.3253	0.9790

where θ is the surface coverage, K is the adsorption–desorption equilibrium constant, C is the concentration of AHAO inhibitor, and g is the adsorbate parameter.

Ultimately, the accuracy of the fit was examined using the correlation coefficient (R^2) given in Table 5.

As can be observed in Table 5, the R^2 values clearly show that data obtained for the Langmuir isotherms are closer to unity than the Langmuir isotherm. Consequently, the set of AHAO inhibitor under study was found to prefer the Langmuir adsorption isotherm.

In our study, it is very important to note that discussion of the adsorption isotherm behavior, using natural product as inhibitors, in terms of the standard free energy of adsorption value, is not possible because the molecular mass of the AHAO constituents is not known. Some authors [45–47], in their study on acid corrosion with natural products, noted the same limitation.

Table 6 Polarization parameters and η_{Tafel} (%) for steel corrosion in 0.5 M H_2SO_4 without and with various concentrations of AHAO at 298 K

C (g L^{-1})	$-E_{corr}$ (mV/SCE)	i_{corr} (μA cm^{-2})	$-\beta_c$ (mV dec^{-1})	η_{Tafel} (%)
Blank	397	2605	226	–
0.65	413	1028	230	60
1.20	415	532	220	80
1.57	428	476	215	82
1.84	458	323	202	87
2.76	547	306	190	88

3.4 Polarization Measurements

Polarization measurements have been carried out in order to gain knowledge concerning the kinetics of the anodic and cathodic reactions. Figure 5 depicts the typical potentiodynamic cathodic and anodic curves of carbon steel electrode after immersion in 0.5 M H_2SO_4 in the absence and presence of various concentrations of AHAO at 298 K. The addition of AHAO to acid solutions shifts both the anodic and cathodic branches of the Tafel plot of the pure acid solution to lower values of current density at all investigated concentrations.

This indicates that AHAO inhibits both hydrogen evolution and metal dissolution and suggests it to act as a mixed type inhibitor. Electrochemical parameters determined from these experiments by extrapolation method [48], as corrosion potential (E_{corr}), corrosion current density (i_{corr}), and cathodic Tafel slopes (β_c), are listed in Table 6. The i_{corr} was determined by Tafel extrapolation of only the cathodic polarization curve alone, which usually produces a longer and better defined Tafel region [48]. The i_{corr} values were used to calculate the inhibition efficiency, η_{Tafel}(%), using the following equation:

$$\eta_{\text{Tafel}}(\%) = \left(\frac{i_0^{\text{corr}} - i^{\text{corr}}}{i_0^{\text{corr}}} \right) \times 100, \quad (7)$$

where i_{corr} and $i_{\text{corr(i)}}$ are the corrosion current densities for steel electrode in the uninhibited and inhibited solutions, respectively.

Inspection of the results in Table 6 shows that the values of corrosion current density (i_{corr}) noticeably decrease in the presence of inhibitor (AHAO), which suggests that rate of electrochemical reaction was retarded due to the formation of a barrier layer on mild surface by adsorption of the AHAO molecules. Moreover, the maximum shift in E_{corr}, compared to that of uninhibited solution, was 150 mV towards cathodic direction indicating therefore that AHAO acts as cathodic-type inhibitor (Fig. 5; Table 6). The cathodic curves (Fig. 5) give rise to parallel lines suggesting that the addition of inhibitor to corrosive environment does not modify the hydrogen evolution mechanism and reduction of H^+ ions at the carbon steel surface follows charge transfer mechanism. The values of β_c in Table 6 show a slight change with increasing inhibitor concentration, indicating the influence of the AHAO inhibitor on the kinetics of hydrogen evolution. The adsorbed protective film of inhibitor on steel surface impedes by blocking the reaction sites of the metal resulted in the significant change of the iron dissolution mechanism [49–51]. In this way, actual surface area available for H^+ ions is decreased while the actual reaction mechanism remains unaffected [51]. The organic compounds existed in the AHAO include functional groups containing large number of heteroatoms like oxygen. As a result, the vacant d-orbital of metal can be interacted with lone pair of electrons of oxygen atoms or π-electron cloud of the donor atoms. The inhibition efficiency values, η_{Tafel} (%), calculated by potentiodynamic polarization method are given in Table 6. The polarization data also confirm the gravimetric results, i.e., AHAO is a good inhibitor and its inhibition efficiency depends on the inhibitor concentration.

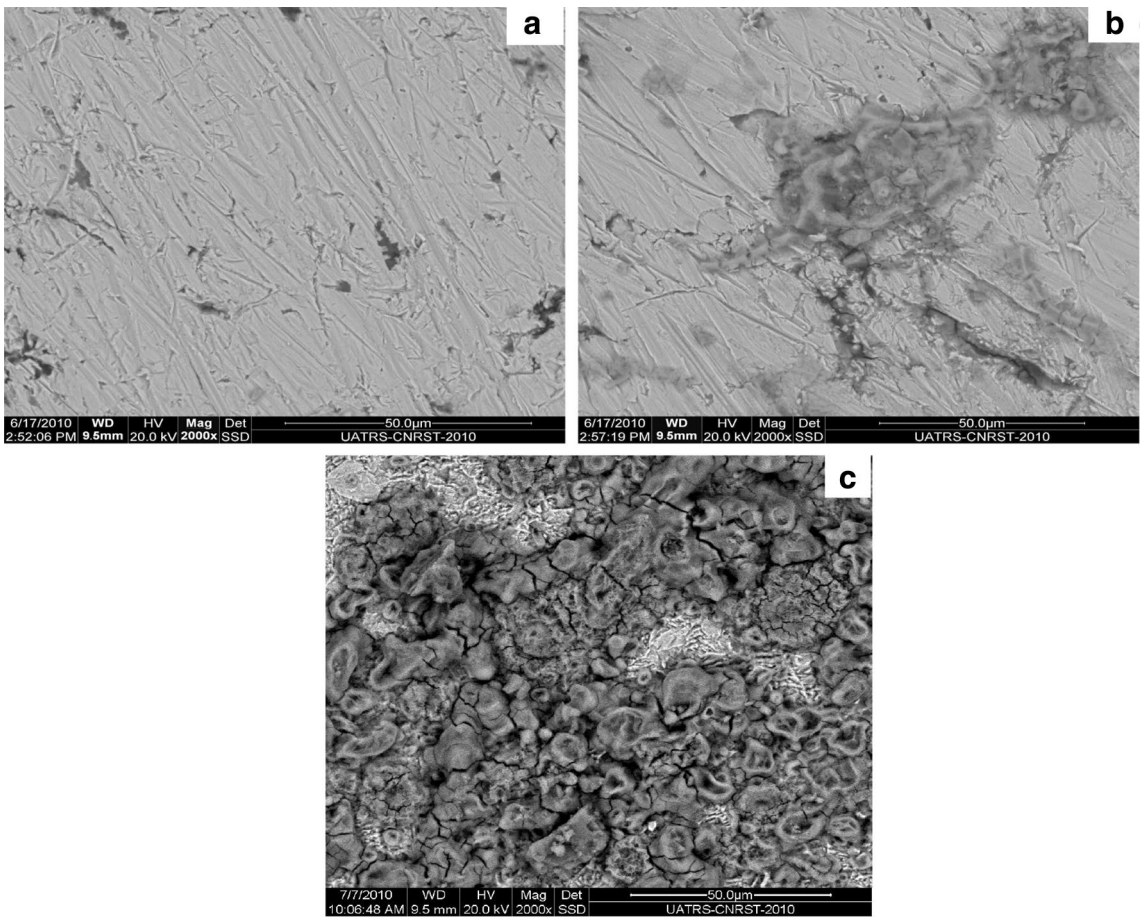

Fig. 6 SEM micrographs of the mild steel surface: **a** metallic surface after being polished, **b** metallic surface after 6 h of immersion in 0.5 M H_2SO_4 with AHAO and **c** metallic surface after 6 h of immersion in 0.5 M H_2SO_4

3.5 Scanning Electron Microscopy (SEM)

The scanning electron micrographs images were recorded in order to confirm the protective film formation during the corrosion process. Figure 6 shows the SEM images of the mild steel surface before and after immersion in 0.5 M H_2SO_4 with and without corrosion AHAO. Figure 6a signifies the SEM image of the polished mild steel surface, except the presence of polishing scratches; the surface shows the absence of noticeable defects such as pits and cracks. Figure 6b, c shows the steel surface after 6 h of immersion in 0.5 M H_2SO_4 without and with AHAO. The resulting of the SEM micrograph shows that the surface was rough and harshly corroded for the reason that the violent attack by 0.5 M H_2SO_4 in the absence of the AHAO. However, there are less pits and cracks observed in the micrographs in the presence of AHAO (Fig. 6b), which suggests a formation of protective film on steel surface which was responsible for the corrosion inhibition. Indeed, AHAO has a strong tendency to adhere to the steel surface and can be regarded as good inhibitor for steel corrosion in sulfuric acid medium. Figure reveals the formation of a protective film of the inhibitor on the mild steel surface which inhibits the corrosion considerably in acidic medium.

4 Conclusions

- The inhibition efficacy of AHAO increases with increasing inhibitor concentration. It reaches a maximal value of 88% at 2.76 g L^{-1} at 298 K.
- The adsorption of the inhibitor on the mild steel surface is correctly described using the Langmuir isotherm.
- Thermodynamic activation parameters were calculated and discussed.

References

1. Kadri A, Ben Chobba I, Zarai Z, Békir A, Néji G (2011) Chemical constituents and antioxidant activity of the essential oil from aerial parts of *Artemisia herba-alba* grown in Tunisian semi-arid region. Afr J Biotechnol 10:2923–2929
2. Segal R, Feuerstein I, Danin A (1987) Chemotypes of *Artemisia herba-alba* in Israel based on their sesquiterpene lactone and essential oil constitution. Biochem Syst Ecol 15:411–416
3. Jouad H, Haloui M, Rhiouani H, El Hilaly J, Eddouks M (2001) Ethnobotanical survey of medicinal plants used for the treatment of diabetes, cardiac and renal diseases in the North centre region of Morocco (Fez-Boulemane). J Ethnopharmacol 77:175–182
4. Tahraoui A, El-Hilaly J, Israili ZH, Lyoussi B (2007) Ethnopharmacological survey of plants used in the traditional treatment of hypertension and diabetes in south-eastern Morocco (Errachidia province). J Ethnopharmacol 110:105–117
5. Zeggwagh NA, Jean Baptiste M, Eddouks M (2014) Acute hypotensive and diuretic activities of *Artemisia herba alba* aqueous extract in normal rats. Asian Pac J Trop Biomed 4:S644–S648
6. Ghanmi M, Satrani B, Aafi A, Isamili MR, Houti H, El Monfalouti H, Benchakroun KH, Aberchane M, Harki L, Boukir A, Chaouch A, Charrouf Z (2010) Effet de la date de récolte sur le rendement, la composition chimique et la bioactivité des huiles essentielles de l'armoise blanche (*Artemisia herba-alba*) de la région de Guerçif (Maroc oriental). Phytothérapie 8:295–301
7. Iriadam MD, Musa GM, Hatice H, Sun Baba F (2006) Effects of two Turkish medicinal plants *Artemisia* herba-alba and Teucrium polium on blood glucose levels and other biochemical parameters in rabbits. J Cell Mol Biol 5:19–24
8. Mighri H, Hajlaoui H, Akrout A, Najjaa H, Neffati M (2010) Antimicrobial and antioxidant activities of *Artemisia herba-alba* essential oil cultivated in Tunisian arid zone. C R Chim 13:380–386
9. Essid R, Rahali FZ, Msaada K, Sghair I, Hammami M, Bouratbine A, Aoun K, Limam F (2015) Antileishmanial and cytotoxic potential of essential oils from medicinal plants in Northern Tunisia. Ind Crops Prod 77:795–802
10. Yashphe J, Feuerstein I, Barel S, Segal R (1987) The antibacterial and antispasmodic activity of *Artemisia herba-alba* Asso. II. Examination of essential oils from various chemotypes. Int J Crude Drug Res 25:89–96
11. Oguzie EE, Li Y, Wang FH (2007) Effect of surface nanocrystallization on corrosion and corrosion inhibition of low carbon steel: synergistic effect of methionine and iodide ion. Electrochim Acta 52:6988–6996
12. Zarrouk A, Zarrok H, Salghi R, Touir R, Hammouti B, Benchat N, Afrine LL, Hannache H, El Hezzat M, Bouachrine M (2013) Electrochemical impedance spectroscopy weight loss and quantum chemical study of new pyridazine derivative as inhibitor corrosion of copper in nitric acid. J Chem Pharm Res 5(12):1482–1491
13. Popova A, Sokolova E, Raicheva S, Christov M (2003) AC and DC study of the temperature effect on mild steel corrosion in acid media in the presence of benzimidazole derivatives. Corros Sci 45:33–58
14. Zarrok H, Zarrouk A, Salghi R, Ebn Touhami M, Oudda H, Hammouti B, Touir R, Bentiss F, Al-Deyab SS (2013) Corrosion inhibition of C38 steel in acidic medium using N-1 naphthylethylenediamine dihydrochloride monomethanolate. Int J Electrochem Sci 8:6014–6032
15. Tayebi H, Bourazmi H, Himmi B, El Assyry A, Ramli Y, Zarrouk A, Geunbour A, Hammouti B (2014) Combined electrochemical and quantum chemical study of new quinoxaline derivative as corrosion inhibitor for carbon steel in acidic media. Der Pharma Chem 6(5):220–234
16. Zarrok H, Salghi R, Zarrouk A, Hammouti B, Oudda H, Bazzi Lh BL, Al-Deyab SS (2012) Investigation of the inhibition effect of N-1-Naphthylethylenediamine dihydrochloride monomethanolate on the C38 steel corrosion in 0.5 M H_2SO_4. Der Pharma Chem 4(1):407–416
17. Tayebi H, Bourazmi H, Himmi B, El Assyry A, Ramli Y, Zarrouk A, Geunbour A, Hammouti B, Ebenso Eno E (2014) An electrochemical and theoretical evaluation of new quinoline derivative as a corrosion inhibitor for carbon steel in HCl solutions. Der Pharm Lett 6(6):20–34
18. Quraishi MA, Singh A, Singh VK, Yadov K, Singh AK (2010) Green approach to corrosion inhibition of mild steel in hydrochloric acid and sulphuric acid solutions by the extract of Murraya koenigii leaves. Mater Chem Phys 122:114–122
19. Nahlé A, El Ouadi Y, Bouyanzer A, Majidi L, Paolini J, Desjobert JM, Costa J, Chahboun N, Zarrouk A, Hammouti B (2016) Evaluation of *Melissa Officinalis* extract and oil as eco-friendly

corrosion inhibitor for carbon steel in acidic chloride solutions. Orient J Chem 32(4):1909–1921
20. Ebenso EE, Eddy NO (2008) Corrosion inhibitive properties and adsorption behaviour of ethanol extract of Piper guinensis as a green corrosion inhibitor for mild steel in H_2SO_4. Afr J Pure Appl Chem 2(11):107–115
21. Boujakhrout A, Hamdani I, Chahboun N, Bouyanzer A, Santana RV, Zarrouk A (2015) Antioxidant activity and corrosion inhibitive behavior of Garcinia cola seeds on mild steel in hydrochloric medium. J Mater Environ Sci 6(12):3655–3666
22. Umoren SA, Obot IB, Ebenzo EE, Obi-Egbedi NO (2008) Synergistic inhibition between naturally occurring exudate gum and halide ions on the corrosion of mild steel in acidic medium. Int J Electrochem Sci 3:1029–1043
23. Salhi A, Bouyanzer A, El Mounsi I, Bendaha H, Hamdani I, El Ouariachi E, Chetouani A, Chahboun N, Hammouti B, Desjobert JM, Costa J (2016) Chemical composition, antioxidant and anticorrosive activities of *Thymus algeriensis*. J Mater Environ Sci 7(11):3949–3960
24. Noor EA (2007) Temperature effects on the corrosion inhibition of mild steel in acidic solutions by aqueous extract of fenugreek leaves. Int J Electrochem Sci 2:996–1017
25. Bouklah M, Hammouti B (2006) Thermodynamic characterisation of steel corrosion for the corrosion inhibition of steel in sulphuric acid solutions by *Artemisia*. Port Electrochem Acta 24:457–468
26. Boumhara K, Bentiss F, Tabyaoui M, Costa J, Desjobert J-M, Bellaouchou A, Guenbour A, Hammouti B, Al-Deyab SS (2014) Use of Artemisia mesatlantica essential oil as green corrosion inhibitor for mild steel in 1 M hydrochloric acid solution. Int J Electrochem Sci 9:1187–1206
27. Adams RP (2007) Junipers of the world: the genus *Juniperus*, 4th edn. Allured Publishing Corporation, Carol Stream
28. König WA, Hochmuth DH, Joulain D (2001) Library of mass finder 2.1. Institute of Organic Chemistry, Hamburg
29. Boutkhil S, El Idrissi M, Chakir S, Derraz M, Amechrouq A, Chbicheb A, El Badaoui K (2011) Antibacterial and antifungal activity of extracts and essential oils of *Seriphidium herba-alba* (Asso) Soják and their combination effects with the essential oils of *Dysphania ambrosioides* (L) Mosyakin & Clemants. Acta Bot Gallica 158(3):425–433
30. Herrag L, Hammouti B, Elkadiri S, Aouniti A, Jama C, Vezin H, Bentiss F (2010) Adsorption properties and inhibition of mild steel corrosion in hydrochloric solution by some newly synthesized diamine derivatives: experimental and theoretical investigations. Corros Sci 52:3042–3051
31. Bentiss F, Lebrini M, Lagrenée M (2005) Thermodynamic characterization of metal dissolution and inhibitor adsorption processes in mild steel/2,5-bis(n-thienyl)-1,3,4-thiadiazoles/hydrochloric acid system. Corros Sci 47:2915–2931
32. Ita BI, Offiong OE (2001) The study of the inhibitory properties of benzoin, benzil, benzoin-(4-phenylthiosemicarbazone) and benzil-(4-phenylthiosemicarbazone) on the corrosion of mild steel in hydrochloric acid. Mater Chem Phys 70:330–335
33. Wahdan MH, Hermas AA, Morad MS (2002) Corrosion inhibition of carbon-steels by propargyltriphenylphosphonium bromide in H_2SO_4 solution. Mater Chem Phys 76:111–118
34. Bockris JO'M, Reddy AKN (1977) Modern electrochemistry, vol 2. Plenum Press, New York, p 1267
35. Elayyachy M, Elkodadi M, Aouniti A, Ramdani A, Hammouti B, Malek F, Elidrissi A (2005) New bipyrazole derivatives as corrosion inhibitors for steel in hydrochloric acid solutions. Mater Chem Phys 93:281–285
36. Szauer T, Brand A (1981) Mechanism of inhibition of electrode reactions at high surface coverages—II. Electrochim Acta 26:1219–1224
37. Guan NM, Xueming L, Fei L (2004) Synergistic inhibition between o-phenanthroline and chloride ion on cold rolled steel corrosion in phosphoric acid. Mater Chem Phys 86:59–68
38. Noor EA, Al-Moubaraki AH (2009) Thermodynamic study of metal corrosion and inhibitor adsorption processes in mild steel/1-methyl-4[4′(-X)-styryl pyridinium iodides/hydrochloric acid systems. Mater Chem Phys 110:145–154
39. Ahamad I, Prasad R, Quraishi MA (2010) Thermodynamic, electrochemical and quantum chemical investigation of some Schiff bases as corrosion inhibitors for mild steel in hydrochloric acid solutions. Corros Sci 52:933–942
40. Popova A, Christov M, Vasilev A (2007) Inhibitive properties of quaternary ammonium bromides of N-containing heterocycles on acid mild steel corrosion. Part I: gravimetric and voltammetric results. Corros Sci 49:3276–3289
41. Bouklah M, Benchat N, Hammouti B, Aouniti A, Kertit S (2006) Thermodynamic characterisation of steel corrosion and inhibitor adsorption of pyridazine compounds in 0.5 M H_2SO_4. Mater Lett 60:1901–1905
42. Ateya B, El-Anadouli BE, El-Nizamy FM (1984) The adsorption of thiourea on mild steel. Corros Sci 24:509–515
43. Ostovari A, Hoseinieh SM, Peikari M, Shadizadeh SR, Hashemi SJ (2009) Corrosion inhibition of mild steel in 1 M HCl solution by henna extract: a comparative study of the inhibition by henna and its constituents (lawsone, gallic acid, α-d-glucose and tannic acid). Corros Sci 51:1935–1949
44. Chauhan LR, Gunasekaran G (2007) Corrosion inhibition of mild steel by plant extract in dilute HCl medium. Corros Sci 49:1143–1161
45. Bobina M, Kellenberger A, Millet JP, Muntean C, Vaszilcsin N (2013) Corrosion resistance of carbon steel in weak acid solutions in the presence of l-histidine as corrosion inhibitor. Corros Sci 69:389–395
46. Gunasekaran G, Chauhan LR (2004) Eco friendly inhibitor for corrosion inhibition of mild steel in phosphoric acid medium. Electrochim Acta 49:4387–4395
47. Li X, Deng S, Fu H (2012) Inhibition of the corrosion of steel in HCl, H_2SO_4 solutions by bamboo leaf extract. Corros Sci 62:163–175
48. Zarrok H, Zarrouk A, Hammouti B, Salghi R, Jama C, Bentiss F (2012) Corrosion control of carbon steel in phosphoric acid by purpald – Weight loss, electrochemical and XPS studies. Corros Sci 64:243–252
49. Li W-h, He Q, Zhang S-t, Pei C-l (2008) Hou B-r, Some new triazole derivatives as inhibitors for mild steel corrosion in acidic medium. Appl Electrochem 38:289–295
50. Ferreira ES, Giacomelli C, Giacomelli FC, Spinelli A (2004) Evaluation of the inhibitor effect of L-ascorbic acid on the corrosion of mild steel. Mater Chem Phys 83:129–134
51. Soltani N, Tavakkoli N, Khayatkashani M, Jalali MR, Mosavizade A (2012) Green approach to corrosion inhibition of 304 stainless steel in hydrochloric acid solution by the extract of *Salvia officinalis* leaves. Corros Sci 62:122–135